# Envelope Hamiltonian of an intense charged-particle beam in periodic solenoidal fields

S.Y. Lee and A. Riabko
*Department of Physics, Indiana University, Bloomington, Indiana 47405*
(Received 27 July 1994)

We introduce a Hamiltonian to describe the Kapchinskij-Vladimirskij envelope equation in the envelope phase space. The envelope Hamiltonian, in the presence of periodic focusing fields, can be decomposed into an unperturbed autonomous Hamiltonian and a time dependent perturbation generated by the remnant focusing field. This periodic perturbation produces families of parametric resonances, which form a tree of bifurcation branches. Each branch follows the tune of the unperturbed Hamiltonian. A prescription for selecting a proper unperturbed Hamiltonian will be discussed.

PACS number(s): 07.77.−n, 29.27.Eg, 41.75.−i, 52.25.Wz

Studies of nonlinear dynamics relevant to the Kapchinskij-Vladimirskij (KV) envelope equation for an intense charged-particle beam are important in order to achieve high current and high brightness beams. In particular, nonlinear properties of the KV equation in a periodic focusing solenoidal field were extensively studied in Refs. [1,2]. There Chen and Davidson derived a KV envelope equation for the equilibrium distribution of an intense charged-particle beam propagating through a periodic solenoidal focusing field. For a mismatched beam, the envelope function presumably obeys the KV equation with a periodic longitudinal modulation. Therefore, solutions of such a KV equation, in the presence of self-electromagnetic fields, can offer important insight toward understanding high brightness beam transport problems.

To solve the nonlinear KV equation with time dependent modulation, Chen and Davidson employed the *Poincaré mapping technique* to systematically determine the dynamics of the envelope oscillations. While numerical simulations are very useful in obtaining a visual chaos for a dynamical system, they often lead to confusion when the number of parameters is large. Sometimes it is difficult to understand the underlying physics based on numerical simulations alone. Furthermore, because correlations between parameters are usually nonlinear, the task of unraveling a key equation is hindered by numerical chaos.

In this Brief Report, we propose a Hamiltonian formalism to describe the KV equation and solve the Hamiltonian flow semianalytically using the parametric resonance analysis method [3]. This paper is organized as follows. The KV envelope equation is reformulated in the *envelope Hamiltonian* and action-angle variables are introduced. Parametric resonances appear naturally when the envelope Hamiltonian is expressed in action-angle variables. Some tracking examples [1], where global chaos occurs, are used to demonstrate the advantage and the applicability of this method.

Following Eq. (46) of Ref. [1], the normalized paraxial KV envelope equation is given by

$$d^2R/ds^2 + k(s)R - K/R - 1/R^3 = 0, \tag{1}$$

where $R$ is the normalized beam radius, $K$ is the normalized space charge perveance factor, $k(s)$ is the normalized linear focusing field, and $s$ is the normalized longitudinal distance along the accelerator. For a periodic focusing field, one has $k(s) = k(s+1)$.

To cast Eq. (1) into a general framework of a periodic dynamical system, such as circular synchrotrons, we use $\theta = 2\pi s$ as the time variable. Let $(R, P)$ be the *envelope phase space* coordinates, where $P$ is conjugate to $R$. The Hamiltonian for Eq. (1) is given by $H = \frac{1}{4\pi}P^2 + V(R)$ with the potential $V(R) = \frac{1}{4\pi}k(\theta)R^2 - \frac{1}{2\pi}K\ln R + \frac{1}{4\pi R^2}$, with $k(\theta) = k(\theta + 2\pi)$. Now we decompose the Hamiltonian into $H = H_0 + \Delta H$ with

$$\begin{aligned} H_0 &= (1/4\pi)P^2 + V_0(R) \\ &= (1/4\pi)P^2 + (1/4\pi)\mu^2R^2 - (1/2\pi)K\ln R \\ &\quad + (1/4\pi R^2), \end{aligned} \tag{2}$$

$$\Delta H = (1/4\pi)[k(\theta) - \mu^2]R^2. \tag{3}$$

The unperturbed autonomous Hamiltonian $H_0$ describes amplitude oscillations of a mismatched beam and the perturbation arises from the remnant of the periodic focusing field. This dynamical system is equivalent to time dependent perturbation on the Hamiltonian flow. We will show later that the parameter $\mu$ should be chosen as the phase advance of the particle motion in the focusing field.

The minimum of the potential well $V_0(R)$ is located at $R_0 = [2/(\sqrt{K^2 + 4\mu^2} - K)]^{1/2}$, which corresponds to the average radius of a matched beam (see the Appendix). Since the autonomous unperturbed Hamiltonian is integrable, a mismatched beam radius will follow a torus of the Hamiltonian flow. The action of the torus is given by

$$J = \frac{1}{2\pi}\oint PdR = \frac{1}{\sqrt{\pi}}\oint [E - V_0(R)]^{1/2}dR, \tag{4}$$

where $E$ is the "energy" of the unperturbed Hamiltonian given by $H_0 = E(J) = \nu J + \frac{1}{2}\alpha J^2 + \cdots$. The tune of the unperturbed Hamiltonian, defined as the number of oscillations in one period, is given by

$$Q(J) = dE/dJ = \nu + \alpha J + \cdots, \tag{5}$$

where the nonlinear detuning parameter

 

$\alpha = (3/64\pi^3 R_0^4\nu^2)(K + 10/R_0^2) - 5/384\pi^5 R_0^6\nu^4(K + 6/R_0^2)^2 + \cdots$ can easily be obtained by the canonical perturbation method and

$$\nu = (1/2\pi)[4\mu^2 - K(\sqrt{K^2 + 4\mu^2} - K)]^{1/2} \quad (6)$$

is the tune at a zero oscillation amplitude of a matched beam. At a zero space charge limit, the phase advance of the unperturbed envelope function in one period is $2\mu$. Since the envelope of a linear system oscillates at twice the particle oscillation amplitude, the parameter $\mu$ should therefore be chosen as the phase advance obtained from a proper Floquet transformation [4] (see also the Appendix). At the infinite space charge limit, the envelope tune becomes $\sqrt{2}\mu$. The nonlinear detuning $\alpha$ arises solely from the space charge force.

Using the generating function $F_2(R, J) = \int_{\hat{R}}^{R} P dR$, where $\hat{R}$ is the maximum amplitude of a Hamiltonian torus, the conjugate phase variable is given by $\psi = \frac{\partial F_2}{\partial J} = 2\pi \frac{\partial E}{\partial J} \int_{\hat{R}}^{R} \frac{dR}{P}$. Although the Hamiltonian $H$ with a periodic time dependent modulation is not integrable, the envelope dynamics can be studied by expanding the perturbing potential in action-angle variables with $R^2 = \sum_{n=-\infty}^{\infty} G_n e^{in\psi}$. Here the strength function $G_n$ is obtained from the inverse Fourier transformation as $G_n = \frac{1}{2\pi}\int_{-\pi}^{\pi} R^2 e^{-in\psi} d\psi$ with $G_{-n} = G_n^*$. Without loss of generality, we assume a symmetric periodic focusing field so that

$$k(\theta) = \sum_{\ell=0}^{\infty} k_\ell \cos \ell\theta. \quad (7)$$

The Hamiltonian becomes

$$H = E(J) + \sum_{n=0,\ell=-\infty}^{\infty} h_{n,\ell} \cos(n\psi - \ell\theta + \gamma_n). \quad (8)$$

where $\gamma_n$ is the phase of $G_n$ and $h_{n,\ell} = k_\ell |G_n|/2\pi$. We neglect first the $n = 0$ terms, which are related to the closed orbit solution (see Appendix). The parametric resonances generated by the time dependent perturbation are given by the stationary phase condition $n\dot{\psi} = \ell$, which can cause coherent perturbation to Hamiltonian tori.

To understand the dynamics of the coherent perturbation, we perform a canonical transformation to the resonance rotating frame using $F_2 = (\psi - \frac{\ell}{n}\theta + \frac{\gamma_n}{n})I$. The time averaged Hamiltonian becomes

$$\langle H \rangle = E(I) - (\ell/n)I + h_{n,\ell}(I) \cos n\phi, \quad (9)$$

where $\phi = \psi - (\ell/n)\theta + \gamma_n/n$ is conjugate to $I$. The fixed points of the Hamiltonian are given by $\sin n\phi_{\rm FP} = 0$ and

$$nQ(I_{\rm FP}) - \ell \pm nh'_{n,\ell}(I_{\rm FP}) = 0, \quad (10)$$

where the prime represents the derivative with respect to the action. Note here that the resonance condition differs from the simple minded condition $nQ(I_{\rm FP}) = \ell$ by the perturbation strength $h'_{n,\ell}$. For the $n$th order resonance, there are $n$ stable fixed points (SFPs) and $n$ unstable fixed points (UFPs). Hamiltonian tori around SFPs are distorted to form resonance islands. The resonance arising from the first order perturbation of Eq. (10) is called the primary $n{:}\ell$ parametric resonance. The width of the resonance is given by $\Delta I = 4(h_{n,\ell}/Q')^{1/2}|_{I=I_{\rm SFP}}$, where $Q'$ is the derivative of the tune.

The occurrence of resonances depends sensitively on the tune of a dynamical system. When the tune is varied by changing system parameters $\mu$ and $K$, the resonance island will also move across the phase space. The bifurcation of resonance islands occurs when the parameters $\mu$ and $K$ are varied such that the solution of Eq. (10) disappears. Plotting the resonance tune vs the energy (or the maximum amplitude of a torus), the dependence of the tune on the amplitude can be obtained. The tree of bifurcation branches for parametric resonances would follow generally the tune of the Hamiltonian [3].

Now we apply the method to an example [1] with

$$k(\theta) = (a_0 + a_1 \cos\theta)^2 = \mu_0^2 + 2a_0a_1 \cos\theta + \frac{1}{2}a_1^2 \cos 2\theta, \quad (11)$$

where $\mu_0 = \sqrt{a_0^2 + a_1^2/2}$. In this example, primary resonances exist only for $\ell = 1$ and 2. When $a_1 \ll a_0$, we can choose $\mu = \mu_0$ for the average phase advance of the periodic focusing field for transverse particle oscillations. However, when $a_1 \gg a_0$, the focusing function is localized and therefore the Floquet transformation may change $\mu$ slightly from $\mu_0$. In the strong thin solenoidal focusing system, the Floquet transformation becomes essential [5].

For the KV equation, when the parameter $\mu_0$ is varied, resonances in the sequences of $n = \ldots, 6, 5, 4, \ldots$ appear at large amplitudes, move across the $(R, P)$ phase space toward $(R_0, 0)$, and bifurcate or disappear. The condition for the $n$th order resonance bifurcation is $\nu = \frac{1}{n}$. For example, the fifth order resonance bifurcates at $\nu \approx \frac{1}{5}$ or equivalently $\mu_0 \approx \frac{\pi}{5}$ for a beam without space charge or $\mu_0 \approx \frac{\sqrt{2}\pi}{5}$ for an intense space charge dominated beam. Similar bifurcation mechanism can be applied to other resonances. In general, higher order resonances, such as $n = 5, 6, 7, \ldots$, are benign because their resonance strengths are small.

Since a large focusing strength $\mu_0$, which needs large $a_0$ and/or $a_1$, is needed to minimize beam radius $R_0$ for beam transport, studies of low order resonances with $n = 4, 3, 2, 1, \ldots$ can be important in optimizing the beam transport. An example of a low order resonance is shown in Fig. 2(b) of Ref. [1], which corresponds to $\nu = 0.297$. Here the third order resonance is located at $3Q(I_r) - 1 + \frac{3}{2\pi}a_0a_1|G_3'(I_r)| = 0$, where $I_r = I_{\rm SFP}$ is the resonance action. When the tune $\nu$ is increased upward, third order resonance islands, shown in Fig. 2(b) of Ref. [1], move in toward the phase space point $(R_0, 0)$. The third order island bifurcates at $\nu = \frac{1}{3}$.

At $\nu \geq 0.4$, Hamiltonian tori are dominated by the 2:1 resonance. This is analogous to the half integer stopband in orbital dynamics of circular synchrotrons, where the stable region around $R_0$ becomes smaller when the tune $\nu$ approaches $\frac{1}{2}$. Near $\nu \approx \frac{1}{2}$, the stability of the envelope equation is similar to that of Mathieu's equation (see the Appendix). The Mathieu instability occurs when the tune lies in the range $\nu \in (\frac{1}{2} - \xi, \frac{1}{2} + \xi)$, where $\xi \approx \frac{a_0a_1}{4\pi^2}$.

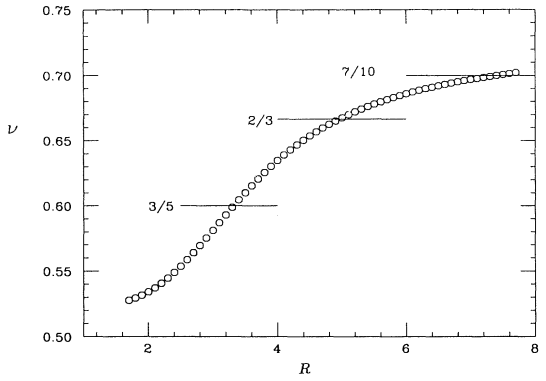


FIG. 1. Tune vs the maximum amplitudes of the unperturbed KV Hamiltonian tori with parameters $\mu_0 = 2.2817$ and $K = 10$. Horizontal lines indicate locations of some resonances.

When the tune is increased further, global chaos becomes an important dynamical issue. A particularly interesting example of near global chaos is shown in Fig. 2(c) of Ref. [1]. In the following, we study the KV Hamiltonian with parameters $\mu_0 = 2.2817$, and $\nu = 0.5256$, which correspond to $a_0 = 1.07, a_1 = 2.85$, and $K = 10$ of Ref. [1]. The tune $Q(J)$ vs the maximum amplitudes $R = \hat{R}$ of the unperturbed Hamiltonian tori is shown as circles in Fig. 1, where some parametric resonances are marked. Note that $Q \in [0.5256, 0.7263)$. For example, the 3:2 primary resonance is expected to occur at a maximum amplitude of $\hat{R} \approx 5$ and the secondary 5:3 resonance will occur at $\hat{R} \approx 3.3$, which is verified in Fig. 2(e). Figure 2 summarizes the stroboscopic maps [6] for $a_1 = 2.85, 2, 1.5, 1$, and 0.5, respectively, while keeping $\mu_0$ constant, where Fig. 2(a) reproduces Fig. 2(c) of Ref. [1] with $a_1 = 2.85$.

Note first that many secondary resonances 7:4, 5:3, and 8:5 appear along with the primary 3:2 resonance in Fig. 2(d) with $a_1 = 1$. These secondary resonances arise from higher order perturbation by combining neighboring harmonics. As the parameter $a_1$ is increased to 1.5 in Fig. 2(c), overlapping 3:2 and 8:5 resonances contribute to the observed chaotic band. We also note interesting tertiary islands around the 3:2 islands. As the parameter $a_1$ is increased to 2, the chaotic band covers most of the envelope phase space. Inside the chaotic sea, only small local islands survive. Here the 4:3 resonance, shown in Figs. 2(a) and 2(b) becomes larger as the parameter $a_1$ is increased. Using Floquet transformation for the case with large $a_1$, the unperturbed tune of Fig. 1 is shifted upward by about 0.05. The inward drift of the 5:3 resonance, the disappearance of the 7:4 resonance, and the existence of 4:3 resonance verify the upward shift of the linear betatron phase advance. When the parameter $a_1$ is reduced to 0.5, shown in Fig. 2(e), the widths of all secondary resonances are small. Because of the initial phase space coordinates used in numerical simulations, the primary 3:2 resonance, which should appear at $R \approx 5$, was not shown on Fig. 2(e).

The physics of nonlinear resonances can be analyzed as the parameter $\nu$ is increased further. Here we would like to study the stability of the unique stable fixed point (USFP) $R_0$ of the KV Hamiltonian [7]. Following the Hamiltonian dynamics, the USFP would disappear when the Mathieu instability occurs at $J = 0$ (see the Appendix). Since the Mathieu resonance strength is proportional to $\frac{a_0 a_1}{4\pi^2}$, Fig. 3 (to be compared with Fig. 5 of Ref. [1]) shows the band of the Mathieu instability for the space charge perveance $K = 0$ and $K = \infty$, respectively, in the parametric space of $(\frac{a_0}{\pi}, \frac{a_1}{\sqrt{2}\pi})$. Similar bands of instabilities also exist at radii of 1, 1.5, 2, .... Along with these first order instabilities, higher order resonances also bifurcate at the USFP at $\nu = \frac{1}{n}$. Some concentric lines at radii of $\frac{1}{n}$ $(n = 3, 4, \ldots)$, shown in Fig. 3, represent the bifurcation points at a zero space charge limit. When $K \neq 0$, all these concentric bands will be shifted outward from the origin.

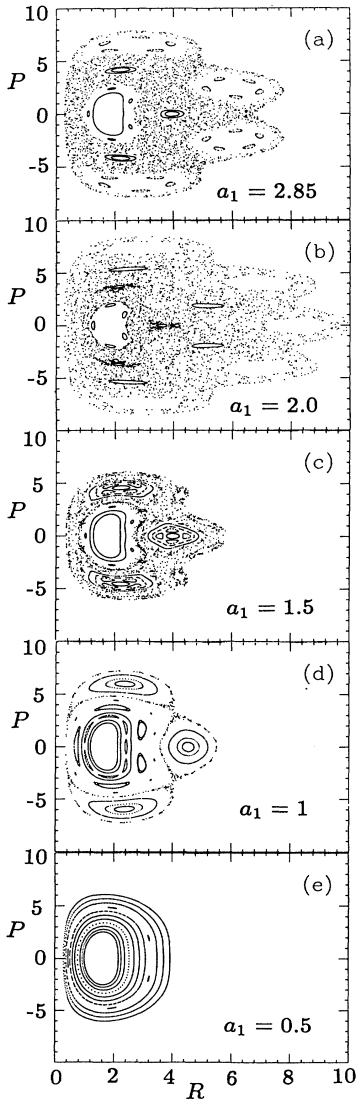


FIG. 2. Stroboscopic maps corresponding to the dynamical system of $\mu_0 = 2.2817, K = 10$ with different $a_1$ parameters. From top to the bottom, the $a_1$ parameters are 2.85, 2.0, 1.5, 1.0, and 0.5, respectively. The stochastic bands shown in plots (a), (b), and (c) arise from overlapping higher order resonances.

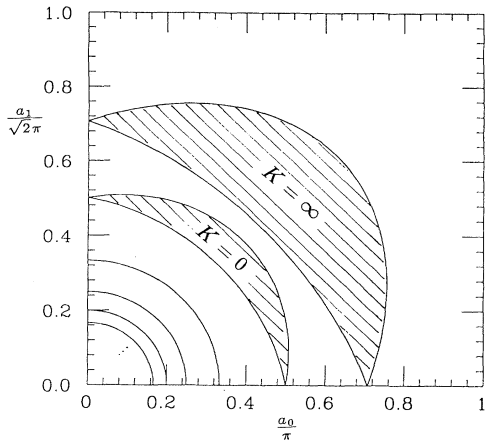


FIG. 3. The parameter space $(a_0/\pi, a_1/\sqrt{2}\pi)$ for the bifurcation of 2:1, 3:1, 4:1, ... resonances. In particular, the instability of $I_{\rm UFP} = 0$ for the 2:1 resonance has a finite width in the parametric space. The parameters corresponding to $K = 0$ and $K = \infty$ are shown for the 2:1 primary resonance. Higher order resonances are shown only for the $K = 0$ scenario.

In conclusion, we have reformulated the KV envelope equation in Hamiltonian dynamics and applied the parametric resonance analysis method to determine the dynamic behavior of the system. Even with a relatively large time dependent perturbation to the KV equation, parametric resonances are well predicted by the Hamiltonian dynamics. Comprehension of the dependence of beam envelope properties on the machine and the beam parameters may lead to an understanding of the mechanism of halo formation, as well as finding methods of prevention.

This work was supported in part by NSF, Grant No. PHY-9221402, and the DOE, Grant No. DE-FG02-93ER40801. We thank R. Ryne for supplying us with a fourth order symplectic integrator during the course of the USPAS at Indiana University.

## APPENDIX: MATHIEU'S INSTABILITIES

The linearized Hamiltonian around $R_0$ is given by

$$H \approx (1/4\pi)P^2 + \pi\nu^2 X^2 + (1/4\pi)[k(\theta) - \mu^2](2R_0 X + X^2) + \cdots, \quad \text{(A1)}$$

where $X = R - R_0$ and $\nu$ is the linear tune of Eq. (5). The linearized equation of motion becomes

$$\ddot{X} + \left[\nu^2 + \frac{1}{4\pi^2}[k(\theta) - \mu^2]\right] X = -\frac{R_0}{4\pi^2}[k(\theta) - \mu^2]. \quad \text{(A2)}$$

For a periodic focusing function of Eq. (11), Eq. (A2) is a driven Mathieu equation. Let the particular (closed orbit) solution of this inhomogeneous equation be $X_{\rm CO}(\theta) = \sum_{n=0}^{\infty} A_n \cos n\theta$, where $A_n$'s are obtained by solving a set of linear equations. The actual radius of the matched beam is given by $R_b = R_0 + X_{\rm CO}(\theta)$ (see Fig. 3 of Ref. [1]). If the parameter $\mu$ is properly chosen, we find that $X_{\rm CO}$ agrees well with the exact equilibrium envelope function obtained by integrating the KV equation [5].

By subtracting the particular solution from Eq. (A2), the stability of the unique stable fixed point of $H_0$ can be obtained from the Mathieu equation

$$\ddot{\tilde{X}} + [\nu^2 + (1/4\pi^2)(k(\theta) - \mu^2)]\tilde{X} = 0, \quad \text{(A3)}$$

where $\tilde{X} = X - X_{\rm CO}$. With the focusing function model of Eq. (11), the condition for the first order Mathieu instability is $4\nu^2 \in (1 - 4\xi, 1 + 4\xi)$, where $\xi \approx \frac{a_0 a_1}{4\pi^2}$. Higher order Mathieu's instabilities are located at $\nu \approx 1, \frac{3}{2}, 2, \frac{5}{2}, \ldots$. Mathieu's instabilities can cause the USFP of $H_0$ to bifurcate.

The first order Mathieu instability is equivalent to the first order parametric resonance. The Hamiltonian near the 2:1 resonance is given by

$$H \approx (\nu - 1/2)I + 1/2\alpha I^2 + (a_0 a_1/8\pi^2\nu) I \cos 2\phi, \quad \text{(A4)}$$

where $G_2 \approx \frac{I}{4\pi\nu}$ is used. The UFP is located at $I_{\rm UFP} = 0$ when $\nu \in (\frac{1}{2} - \xi, \frac{1}{2} + \xi)$, which, to the first order in $\xi$, is equivalent to the Mathieu first order instability. The Hamiltonian formalism, which includes the nonlinear detuning term $\alpha$, can be used to find $I_{\rm SFP}$.

[1] C. Chen and R.C. Davidson, Phys. Rev. E **49**, 5679 (1994).
[2] C. Chen and R.C. Davidson, Phys. Rev. Lett. **72**, 2195 (1994).
[3] S.Y. Lee *et al.*, Phys. Rev. E **49**, 5717 (1994).
[4] E.D. Courant and H.S. Snyder, Ann. Phys. (N.Y.) **3**, 1 (1958).

[5] When the focusing element in a beam transport system is localized, such as the thin lens or piecewise constant solenoidal field with strong focusing, the Floquet transformation is need to obtain a proper $\mu$ in order to obtain an good representation of the closed orbit envelope function. If $\mu$ were not chosen properly, then the resonance strength function $G_n$ would be distributed differently and a higher order canonical perturbation method would have to be applied to obtain the proper tune of the system. Figure 4 of Ref. [2] is an excellent example, where $\mu = 115°$ is chosen, and therefore the envelope tune $Q_e$ lies between 0.4788 and 0.6388. This means that the system should exhibit a dominant 2:1 resonance. However, Fig. 4 of Ref. [2] shows only 3:2, 7:5, and 4:3 resonances, where the 4:3 resonance is misidentified as the 4:2 resonance. All these resonances should be outside the envelope tune range. Using the Floquet transformation, we obtain $\mu = 144.7°$. Thus the actual envelope tune lies in the range of 0.6159 – 0.8021. The 3:2, 7:5, and 4:3 resonances observed in Fig. 4 of Ref. [2] fall naturally within the range of the envelope tune.

[6] In order to obtain the stroboscopic maps, we perform numerical simulations using a fourth order symplectic integration to the differential equation $\dot{R} = \frac{1}{2\pi}P$, $\dot{P} = -\frac{1}{2\pi}k(\theta)R + \frac{K}{2\pi R} + \frac{1}{2\pi R^3}$, where overdots are derivatives with respect to $\theta$. The stroboscopic map is obtained by plotting one phase space point at every $\theta = 2\pi$ time interval.

[7] The SFPs discussed in Eq. (9) are fixed points in the stroboscopic maps. Since these stroboscopic maps are rotating about the $I = 0$ phase space point at a periodic time interval, they are not fixed points for all times. The USFP $H_0$ is $R_0$, which does not move when the phase space is rotated. In reality, the envelope function for a matched beam in a periodic focusing field is given by $R_b = R_0 + X_{\rm CO}(\theta)$ (see the Appendix), which also depends on time.